Eur Respir J 2000; 15: 570–578
Printed in UK – all rights reserved

Copyright ©ERS Journals Ltd 2000
European Respiratory Journal
ISSN 0903-1936

Detection of inspiratory flow limitation during sleep by computer assisted respiratory inductive plethysmography

V. Kaplan, J.N. Zhang, E.W. Russi, K.E. Bloch

Detection of inspiratory flow limitation during sleep by computer assisted respiratory inductive plethysmography. V. Kaplan, J.N. Zhang, E.W. Russi, K.E. Bloch. ©ERS Journals Ltd 2000.

ABSTRACT: The potential of respiratory inductive plethysmography (RIP) to detect inspiratory flow limitation during sleep was investigated.

Sixteen sleep apnoea patients underwent polysomnography. Airflow by a flowmeter attached to a nasal mask, oesophageal and mask pressure were recorded along with calibrated RIP. Presence of inspiratory flow limitation was defined by constant or decreasing flow without pressure dependence throughout significant portions of inspiration, its absence by a linear or mildly alinear pressure:airflow relationship. Based on this standard, three of various computerized RIP derived parameters, with highest performance to detect flow limitation, were identified. They were combined to an inspiratory flow limitation, (IFL)-Index(RIP), which was validated prospectively in another 10 sleep apnoea patients.

RIP derived fractional inspiratory time, peak to mean inspiratory flow ratio, and ribcage contribution to tidal volume had the highest accuracy to detect flow limitation (area under the receiver operating characteristic (ROC) curves 0.81, 0.76, 0.76, respectively, 160 comparisons). Prospective validation revealed an area under the ROC curve for the IFL-Index(RIP) to detect flow limitation of 0.89 (95% confidence interval 0.85 to 0.93, 200 comparisons) with sensitivity and specificity at the point of equality of 80%.

It is concluded that inspiratory flow limitation may be assessed by computer assisted analysis of respiratory inductive plethysmography derived breathing patterns with clinically acceptable accuracy.

Eur Respir J 2000; 15: 570–578.

Pulmonary Division, Dept of Internal Medicine, University Hospital of Zürich, Zürich, Switzerland.

Correspondence: K.E. Bloch, Pulmonary Division, Dept of Internal Medicine, University Hospital of Zürich, CH-8091 Zürich, Switzerland. Fax: 41 12554451

Keywords: Flow limitation
noninvasive monitoring
respiratory inductive plethysmography
sleep apnoea
sleep disturbance
upper airway

Received: November 10 1998
Accepted after revision November 12 1999

This work was supported by grants from the Lungenliga des Kantons Zürich, Switzerland.

In patients with obstructive sleep apnoea syndrome, obvious apnoeas/hypopnoeas with oxygen desaturation may be assessed by an oral-nasal thermistor or a nasal pressure sensor, recordings of chest wall motion, and pulse oximetry [1, 2]. If quantitative estimation of ventilation, airway resistance or inspiratory flow limitation is required for detection of subtle breathing disturbances, such as occur in the "upper airway resistance syndrome", measurement of airflow by a flow meter attached to a tightly fitting mask, and recording of oesophageal or pharyngeal pressure by a catheter have been essential [3–5]. However, such instrumentation may disturb sleep and ventilation, and is uncomfortable for the patient.

Rib cage and abdominal volume curves, recorded noninvasively by calibrated respiratory inductive plethysmography (RIP), have been shown to estimate airflow at the oral-nasal orifice in normal subjects during natural breathing and application of continuous negative airway pressure [6]. Furthermore, rib cage-abdominal asynchrony and paradoxical motion quantified by RIP reflect increased inspiratory loading as suggested in normal subjects during breathing with added external loads [6, 7], and in patients with obstructive sleep apnoea syndrome (OSAS) during sleep disruptive snoring [6]. Rib cage-abdominal paradox, assessed qualitatively from noncalibrated piezoelectric chest wall motion sensors has been evaluated as a means for assessment of adequate continuous positive airway pressure (CPAP) treatment [8]. In a more recent investigation [9], changes in the contour of the differentiated RIP sum signal (V'_{RIP}) were analyzed for their potential to indicate inspiratory flow limitation. In 7 nonobese habitual snorers, an index derived from the time profile of V'_{RIP} revealed a sensitivity and specificity of 71% in differentiating absent or mild from moderate or severe inspiratory flow limitation [9]. Rib cage-abdominal asynchrony was not analyzed.

In the current study, the purpose was to expand upon this work by using the combined information obtained from calibrated RIP derived flow-time, flow-volume, and rib cage-abdominal volume curves to improve accuracy in detection of inspiratory flow limitation. Furthermore, our goal was to develop and validate an algorithm that allows automated detection of inspiratory flow limitation by computer assisted RIP that is not subject to the potential observer bias of tedious "visual" analysis.

To this end, various numerical RIP derived descriptors of breathing patterns, were systematically evaluated for their potential to detect inspiratory flow limitation in a group of patients with the OSAS during polysomnography. Recordings of oesophageal pressure and airflow by a flow

meter served as the standard to determine the extent of flow limitation. Based on the results of these learning sessions, the RIP derived parameters with the best diagnostic performance were determined. Subsequently, their accuracy in discrimination of presence from absence of inspiratory flow limitation was prospectively tested in another sample of sleep apnoea patients.

Methods

Learning sessions

These served to evaluate the potential of various computer assisted RIP derived breathing pattern parameters for detection of inspiratory flow limitation in comparison to the invasive standard based on oesophageal pressure and airflow recordings.

Patients. Sixteen male patients with OSAS, median age (range) 49 yrs (35–62 yrs), median body-mass-index (range) 31 $kg \cdot m^{-2}$ (22–53 $kg \cdot m^{-2}$), median apnoea-hypopnoea-index (range) 42·h^{-1} (10–116·h^{-1}) were studied. Informed consent and the approval of the hospital review committee for human studies were obtained.

Protocol. Eleven patients, who had been on CPAP therapy for at least two weeks, underwent CPAP titration during full night polysomnography. At the beginning of the night, mask pressure was set at the individual therapeutic level determined previously. When the patient had reached stage II non-rapid eye movement (REM) sleep, mask pressure was reduced by 1 $cmH_2O \cdot min^{-1}$ until arousals or apnoeas occurred. Mask pressure was then increased by 1 $cmH_2O \cdot min^{-1}$ until arousals occurred. If wakefulness occurred before a titration run was completed, the original therapeutic CPAP level was restored. Titration was resumed when the patient had reached stage II non-REM sleep again. In each patient at least three titration runs were completed. In five other patients diagnostic polysomnography without application of any treatment was performed.

Measurements. Polysomnography (Alice 3; Healthdyne Technologies, Marietta, GA, USA) included two electroencephalogram channels (C4/A1, C3/A2), left and right electro-oculogram, submetal electro-myogram, body position, snoring sounds, computer assisted calibrated RIP (Respitrace PT; Noninvasive Monitoring Systems Inc., Miami Beach, FL, USA) [6], and nasal airflow (V'_{FM}) recorded by an ultrasound transit time flowmeter [10] (Spiroson; Isler Bioengineering, Dürnten, Switzerland) interposed between a tightly fitting nasal mask and the leak valve (WhisperSwivel; Respironics Inc., Murrysville, PA, USA) of the CPAP circuit. In studies without CPAP application, a nasal mask was fitted with the flowmeter attached to it but without CPAP circuit. Oesophageal pressure was monitored by means of a balloon catheter placed according to standard techniques [11]. Oesophageal and nasal mask pressure were measured with differential pressure transducers (Validyne, Northridge, CA, USA). Absence of mouth breathing was verified by video monitoring using a low light video camera and an infrared light source.

At the beginning of the studies, the relative gain of the rib cage and abdominal RIP channels were determined with the qualitative diagnostic calibration (QDC) procedure during 5 min of natural breathing [12]. Subsequently, the RIP sum signal was calibrated in absolute volume units (L) by comparison to the integrated output of the flowmeter >20–30 breaths. Validation of RIP calibration in the morning at the end of the sleep studies revealed an accuracy of RIP derived tidal volumes within 12.5% of corresponding values measured by the flow meter in all patients.

Data analysis. Sleep staging. Sleep stages and arousals were "manually" scored according to standard criteria by review of 30 s epochs on a high resolution computer video screen [13, 14].

Breathing pattern analysis. In the recording of each patient, five periods containing 5–7 breaths with relatively high pleural pressure swings (mean±SD 13.1±5.2 cmH_2O), and five periods with relatively low pleural pressure swings (mean±SD 2.3±1.5 cmH_2O) were identified during non-REM sleep. These data represented the learning sample consisting of 160 periods of 5–7 breaths. For each period medians of breathing pattern parameters quantifying timing, volume/flow, and rib cage-abdominal coordination (table 1 and figure 1 [6, 15–18]) were automatically computed using specialized software (RespiEvents EDP, version 4.2a; Non Invasive Monitoring Systems Inc., Miami Beach, FL, USA).

Grading of inspiratory flow limitation by the invasive standard. The extent of inspiratory flow limitation was determined based on time series plots of airflow (V'_{FM}, derived by flowmeter) and transpulmonary pressure (P_{tp}= difference between mask and oesophageal pressure), and on plots of flow *versus* resistive pressure. Resistive pressure (P_{res}) was derived from transpulmonary pressure by subtracting elastic recoil pressure of the lungs (P_{el}) as a signal proportional to volume (V_L) [19]:

$$P_{res} = P_{tp} - P_{el} = P_{tp} - V_L \times E_L$$

The proportionality constant (E_L) reflects lung elastance or its reciprocal, compliance. It was determined during tidal breathing by setting resistive pressure at end-inspiratory and end-expiratory points of no flow to zero, *i.e.* by dividing the difference in P_{tp} between end-inspiration and end-expiration by tidal volume.

Based on a scale similar to that proposed by CLARK *et al.* [9], each of the 160 periods of 5–7 breaths were categorized into one of four inspiratory flow limitation levels. The levels were defined by visual inspection of the time series plots and the flow *versus* pressure plots. Level 1 and 2 corresponded to a linear or mildly alinear pressure: flow relationship; level 3 and 4 corresponded to a constant or decreasing flow rate with no or negative pressure dependence throughout significant portions of inspiration (fig. 2). To evaluate the intra- and inter-observer variability in visually scoring flow limitation, a set of 35 periods of 5–7 breaths were scored twice by the same and once by a second observer. Intra- and inter-observer agreement in scoring of 4 inspiratory flow limitation levels was 77% and 57%, only. Thus we collapsed levels 1 and 2 into one category ("flow limitation absent") and levels 3 and 4 into

Table 1. – Breathing pattern parameters derived by computer assisted respiratory inductive plethysmography

Breathing pattern component	Parameter	Abbreviation	Unit	Description	[Ref.]
Timing	Respiratory rate	f_R	min^{-1}	Number of breaths cycles per minute determined breath by breath	[15]
	Inspiratory time	t_I	s	Interval from end-expiration to end-inspiration	
	Fractional inspiratory time	t_I/t_{tot}		Ratio of inspiratory time to respiratory cycle time	
Volume/Flow*	Tidal volume	V_T	L	Inspiratory tidal volume	
	Minute ventilation	V'_I	$L \cdot min^{-1}$	Inspiratory minute ventilation	
	Mid-inspiratory to mid-expiratory flow ratio	IE50		Ratio of inspiratory to expiratory flow at 50% of tidal volume	[18]
	Peak tidal inspiratory to peak tidal expiratory flow ratio	PTIF/PTEF		Ratio of peak inspiratory to peak expiratory flow during tidal breathing	[16]
	Peak tidal inspiratory to mean tidal inspiratory flow ratio	PTIF/MTIF		Ratio of peak inspiratory to mean inspiratory flow during tidal breathing	[16]
Co-ordination of rib cage-abdominal motion	Rib cage contribution to tidal volume	V_{RC}/V_T		Ratio of rib cage tidal volume of RIP sum signal	
	Phase angle	Phase Angle	Degrees	Phase shift between rib cage and abdominal motion	[17]
	Phase relation	PhaseRel	%	Fraction of the breathing cycle (%) during which rib cage and abdomen move in opposite direction	
	Laboured breath index	LBI		Areas under the inspiratory time derivatives of ribcage and abdomen divided by the area under the time derivative of the sum signal	[15]

*: airflow (V'_{RIP}) was estimated by RIP from the time derivative of the sum signal (volume rib cage + abdomen).

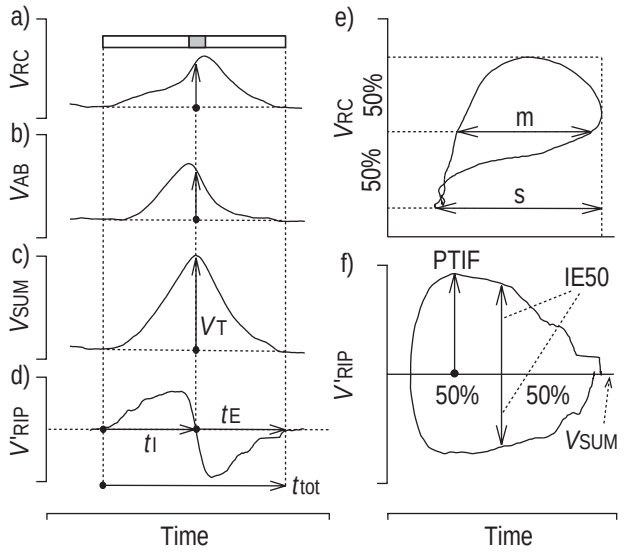

Fig. 1. – Breathing pattern parameters derived by respiratory inductive plethysmography (RIP) are illustrated in time series (a–d); e) rib cage *versus* abdominal volume loops; and f) flow *versus* volume plots. V_{RC}: rib cage volume; V_{AB} abdominal volume; V_{SUM}: sum of rib cage and abdominal volume; V'_{RIP}: time derivative of V_{SUM}. In the time series plot, vertical dotted lines mark beginning and end of inspiration and expiration, horizontal dotted lines mark end-expiratory volumes and zero flow, respectively. The shaded area of the horizontal bar represents Phase Relation, the fraction of the breathing cycle during which ribcage and abdomen move in opposite direction. In the ribcage *versus* abdominal volume plot (e), the horizontal dotted lines mark end-expiratory, mid- and end-inspiratory ribcage volumes, the vertical dotted line represents end-inspiratory abdominal volume. Abbreviations and calculation of parameters are explained in table 1.

another category ("flow limitation present") for the subsequent sensitivity/specificity analysis (see below). Intra- and inter-observer agreement in scoring the two main categories inspiratory flow limitation "present" or "absent" was 97.1% and 94.3%, respectively.

Validation sessions

These served to prospectively validate the diagnostic performance of those RIP derived breathing pattern parameters that had been identified in the learning sessions as discriminating best among presence (levels 3 and 4) and absence (levels 1 and 2) of inspiratory flow limitation.

Patients. Ten patients (1 female) with OSAS, median age 56 yrs (41–71 yrs), median body-mass-index 30 $kg \cdot m^{-2}$ (24–38 $kg \cdot m^{-2}$), median apnoea-hypopnoea-index $56 \cdot h^{-1}$ ($49–65 \cdot h^{-1}$) underwent polysomnographic CPAP titration studies with informed consent and with approval of the hospital review committee for human studies. None of these patients had participated in the learning sessions.

Protocol and measurements. CPAP titration protocol and measurements were identical as in the learning sessions.

Data analysis. Breathing pattern analysis by computer assisted RIP and the flow limitation standard were the same as in the learning sessions. For each patient, 20 periods of 5–7 breaths with either relatively low (mean±SD 2.4±3.4 cmH_2O) and relatively high (16.3±7.1 cmH_2O) oesophageal pressure swings were analyzed during non-REM sleep. Thus, the test sample consisted of 200 periods of 5–7 breaths.

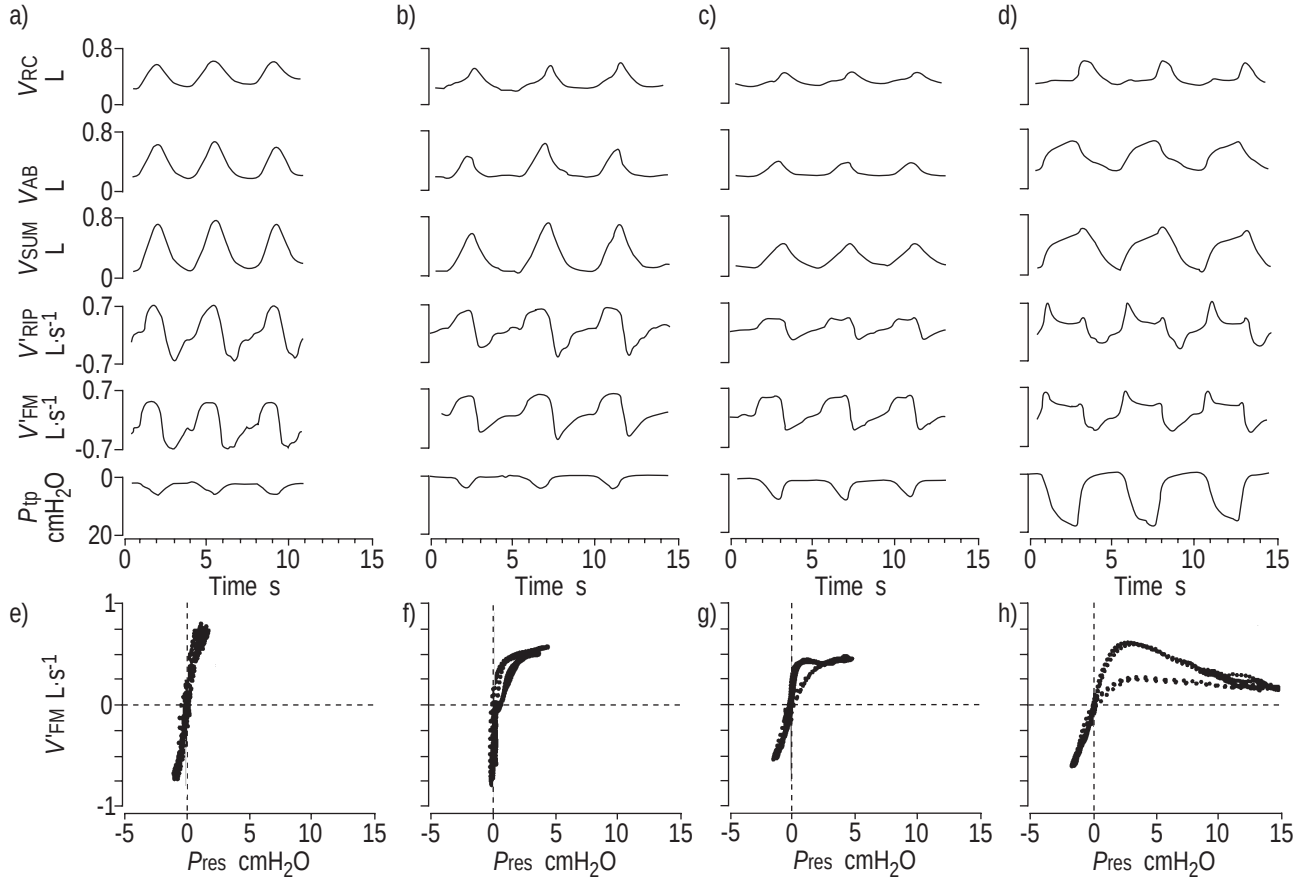

Fig. 2. – Respiratory inductive plethysmography (RIP) derived waveforms are displayed along with airflow recorded with a flow meter attached to a nasal mask, and transpulmonary pressure. Based on review of time series of pressure and airflow recordings (a–d), and on the resistive pressure:flow relationship (e–h), an ordinal scale for inspiratory flow limitation was defined:linear pressure:flow relationship (level 1 (a, e)), mildly alinear relationship (level 2 (b, f)), constant flow rate with no pressure dependence during major portion of inspiration (level 3 (c, g)), and decreasing flow rate with no or negative pressure dependence during major portion of inspiration (level 4 (d, h)). Levels 1 and 2 were designed as "flow limitation absent", levels 3 and 4 as "flow limitation present". With progression of flow limitation, changes in the shape of the differentiated RIP sum, and desynchronization of rib cage-abdominal motion occur. V_{RC}: ribcage volume; V_{AB}: abdominal volume; V_{SUM}: sum of rib cage and abdominal volume; V'_{RIP}: time derivative of V_{SUM}; V'_{FM}: nasal airflow measured by flow meter; P_{tp}: transpulmonary pressure; P_{res}: resistive pressure.

Statistics. Continuous data are summarized as means, SD, and 95% confidence intervals [20]. A statistically significant difference among means was defined by a p value of <0.05. The performance of RIP in detection of inspiratory flow limitation in comparison to the gold standard consisting of the airway pressure:flow relationship was assessed by receiver operating characteristics [21].

Results

Learning sessions

Table 2 provides a summary of the values of various RIP derived breathing pattern parameters during periods of presence (levels 3 and 4) and absence (levels 1 and 2) of inspiratory flow limitation as determined by pressure and flow recordings in 16 OSAS patients. Areas under the receiver operating characteristic (ROC) curves for discrimination of flow limited from not flow limited breaths are also provided for each RIP parameter (table 2). During ascending and descending CPAP titration runs RIP derived breathing pattern parameters tracked changes in inspiratory flow limitation as illustrated in figure 3. There was hysteresis in the change of breathing pattern parameters relative to changes in CPAP level (fig. 4).

To obtain an RIP derived measure of inspiratory flow limitation that incorporated information from several breathing pattern components (timing, volume/flow, rib cage-abdominal coordination), the parameters with the highest areas under the ROC curve were determined for each of these three components. Only parameters available after QDC during natural breathing [12] without requirement for RIP calibration in absolute volume units (L) by a spirometer or flow meter were included in this analysis. The three parameters were fractional inspiratory time (t_I/t_{tot}), peak tidal inspiratory to mean tidal inspiratory flow ratio (PTIF/MTIF), and rib cage contribution to tidal volume (V_{RC}/V_T) (table 2). They were combined to an inspiratory flow limitation index [IFL-Index(RIP)] by building the product of their normalized values (denoted by the subscript "N"):

$$\text{IFL}-\text{Index(RIP)} = t_I/t_{tot_N} \times \text{PTIF/MTIF}_N \times V_{RC}/V_{T_N}$$

Normalization of the index components aimed at providing a similar weight despite different orders of magnitude of raw values. Normalization was achieved by

Table 2. – Learning sample: respiratory inductive plethysmography derived breathing pattern parameters for detection of inspiratory flow limitation

Breathing pattern component	Breathing pattern parameter	Unit	Inspiratory flow limitation by analysis of pressure and airflow		
			"Absent" (level 1+2) n=76	"Present" (levels 3+4) n=84	Discrimination n=160
Timing	t_I/t_{tot}		0.40±0.04 (0.39–0.41)	0.47±0.08 (0.45–0.49)*	0.81 (0.75–0.87)‡§
Volume/flow	V'_I	L·min^{-1}	7.8±5.7 (6.5–9.1)	8.6±6.6 (7.2–10.0)	0.48 (0.40–0.56)
	IE50		1.10±0.26 (1.04–1.16)	0.90±0.32 (0.83–0.97)*	0.73 (0.66–0.80)‡
	PTIF/PTEF		0.98±0.2 (0.94–1.03)	1.02±0.3 (0.95–1.08)	0.48 (0.40–0.56)
	PTIF/MTIF		1.28±0.1 (1.25–1.30)	1.52±0.29 (1.45–1.58)*	0.76 (0.69–0.83)‡§
Co-ordination of rib cage-abdominal motion	V_{RC}/V_T		0.38±0.16 (0.34–0.41)	0.60±0.31 (0.53–0.67)*	0.76 (0.69–0.83)‡§
	Phase Angle	Degrees	31±27 (25–37)	46±42 (37–55)*	0.60 (0.52–0.68)‡
	PhaseRel	%	20±16 (17–24)	24±19 (20–28)	0.55 (0.48–0.62)
	LBI		1.11±0.15 (1.08–1.15)	1.29±0.37 (1.21–1.37)*	0.66 (0.58–0.74)‡
	IFL-Index (RIP)		0.39±0.09 (0.37–0.41)	0.71±0.35 (0.64–0.79)*	0.90 (0.85–0.95)‡

Data presented as mean±SD (95% confidence interval (CI)) or area under receiver operating characteristic curve (95% CI), from recordings in 16 patients. See methods for definition of inspiratory flow limitation levels 1–4 based on airflow and pressure analysis. *: $p<0.05$ *versus* "absent" flow limitation; ‡: 95% CI not overlapping 0.5; §: parameters combined to inspiratory flow limitation index [IFL-Index(RIP)], see text for description.

conversion of the observed range of values to a range of 0.5–1.5 (dimensionless) by linear transformation.

Observed ranges for t_I/t_{tot}, PTIF/MTIF, and V_{RC}/V_T were 0.2 to 0.6, 1.0 to 2.5 and 0 to 1.5, respectively. Thus, the conversion of raw to normalized values was obtained by the following equations:

$$t_I/t_{tot_N} = 0.5 + 1/(0.6 - 0.2) \times (t_I/t_{tot} - 0.2)$$

$$\mathrm{PTIF/MITF_N} = 0.5 + 1(2.5 - 1.0) \times (\mathrm{PTIF/MTIF} - 1.25)$$

$$V_{RC}/V_{T_N} = 0.5 + 1/(1.5 - 0) \times (V_{RC}/V_T - 0)$$

The ROC curves for the individual and combined components of the IFL-Index(RIP) are displayed in figure 5. The area under the ROC curve of the IFL-Index(RIP) for discrimination of presence from absence of flow limitation was 0.90, 95% CI 0.85–0.95, thus greater than any of the areas of its components individually (table 2). For a cut-off value of 0.48, sensitivity and specificity were 83% and 83%, respectively (fig. 5).

Prospective validation sessions

In 10 additional OSAS patients the diagnostic performance of the three parameters t_I/t_{tot}, PTIF/MTIF, and V_{RC}/V_T individually, and combined to the IFL-Index(RIP) was tested prospectively to validate their diagnostic performance. The areas under ROC curves for detection of inspiratory flow limitation were similar to those in the training sessions (table 3, figure 6). The sensitivity and specificity of the IFL-Index(RIP) at the point of equality was 80%.

To investigate whether changes in body position affected accuracy of the IFL-Index(RIP) for detection of inspiratory flow limitation, the data were analyzed separately for supine and lateral body position. The areas under the ROC curves for the IFL-Index(RIP) were 0.82 (95% CI 0.77–0.87) for supine position (n=145 periods), and 0.88 (0.82–0.94) for lateral body position (n=55 periods). The difference was not statistically significant.

Discussion

RIP is widely used for monitoring respiration during sleep since it has the advantage over direct measurement of airflow by a flow meter to be not dependent on airway instrumentation. If operated in a calibrated mode RIP allows detection of apnoeas/hypopnoeas as well as classification of such events as either obstructive or central by the presence or absence of breathing efforts reflected in rib cage-abdominal motion. In the current study, the potential application of RIP was extended to detect inspiratory flow limitation. Based on systematic evaluation in a series of learning sessions, the RIP derived parameters, which best reflected inspiratory flow limitation, were identified. A series of prospective validation studies, performed in another group of patients, confirmed a relatively high accuracy of computer assisted automated analysis of RIP derived breathing patterns, to detect presence or absence of moderate to severe inspiratory flow limitation, in comparison to analysis of pressure and airflow recordings.

The standard for quantification of inspiratory flow limitation

The analysis was based on the standard of invasive pressure and airflow measurements. Unlike CLARK *et al.* [9] who computerized the shape analysis of the pressure:-flow relationship, we performed a qualitative grading of flow limitation by visual inspection. The high intra- and inter-observer agreement in flow limitation scores of 97.1% and 94.3%, respectively, suggests that the bias introduced by the visual as opposed to the more objective computerized analysis was not a major problem.

The flow *versus* resistive pressure plots were derived from transpulmonary rather than from transpharyngeal pressure. Therefore, flow limitation of both, upper and lower airways was assessed. This seems justified in terms of physiological significance, since increased pleural pressure swings, one of the triggers for arousals [22], reflect

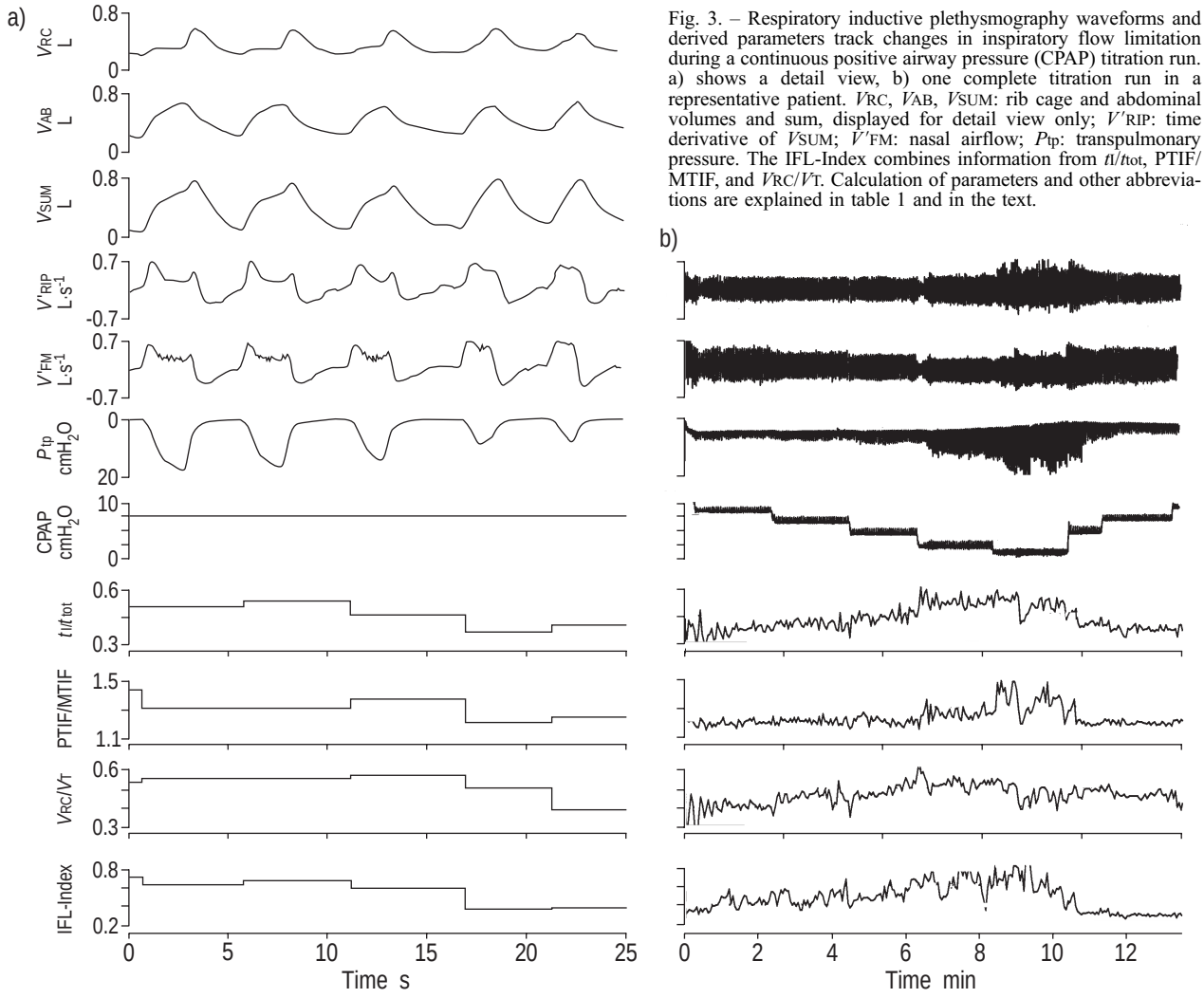

Fig. 3. – Respiratory inductive plethysmography waveforms and derived parameters track changes in inspiratory flow limitation during a continuous positive airway pressure (CPAP) titration run. a) shows a detail view, b) one complete titration run in a representative patient. V_{RC}, V_{AB}, V_{SUM}: rib cage and abdominal volumes and sum, displayed for detail view only; V'_{RIP}: time derivative of V_{SUM}; V'_{FM}: nasal airflow; P_{tp}: transpulmonary pressure. The IFL-Index combines information from t_I/t_{tot}, PTIF/MTIF, and V_{RC}/V_T. Calculation of parameters and other abbreviations are explained in table 1 and in the text.

resistance of upper and lower airways (in addition to elastic forces overcome during inspiration).

By reducing the grading scale for flow limitation to two main categories, "flow limitation absent or mild" and "moderate to severe", assessment of the performance of RIP to estimate flow limitation was unable to be carried out in a more quantitative way. However, the potential of a non-invasive technique to differentiate mild degrees of inspiratory flow limitation, that occur during normal sleep [4], from the more severe forms observed in patients with respiratory sleep disturbances [5], may still be relevant and clinically useful, since RIP provides this information automatically and without requirement for airway instrumentation.

Characteristics of RIP derived breathing patterns during inspiratory flow limitation

Consistent with the well known effects of inspiratory flow limitation on the shape of the flow contour [23], the differentiated RIP sum signal (V'_{RIP}) assumed a flattened appearance. The effects of a reduction in inspiratory flow on ventilation were alleviated by an increase in fractional inspiratory time (table 2). The contour of V'_{RIP} closely but not entirely matched the contour of airflow measured by the flowmeter (V'_{FM}) (fig. 2). Characteristically, a brief prominent peak in V'_{RIP} was observed in early inspiration with higher degrees of flow limitation. This translated into high values for PTIF/MTIF and may have prevented a significant reduction of PTIF/PTEF (table 2). The inspiratory V'_{RIP} peak was generally more pronounced than the corresponding V'_{FM} peak (fig. 7), suggesting that decompression of air without effective flow in the upper airway [24, 25], and deformation of the chest wall during rigorous breathing efforts [17] took place.

Resistance to inspiratory flow increased asynchronous and paradoxical motion of rib cage and abdomen (increased phase angle and Labored Breathing Index, table 2). This nonspecific sign of unfavourable relation between respiratory load and available strength of respiratory muscles has been observed during sleep disruptive snoring in patients with OSAS [6], and during breathing with added external loads in normal subjects [6, 7]. Predominant thoracic breathing (V_{RC}/V_T >0.5) suggested that accessory respiratory muscles assisted inspiration during flow limitation [3, 26].

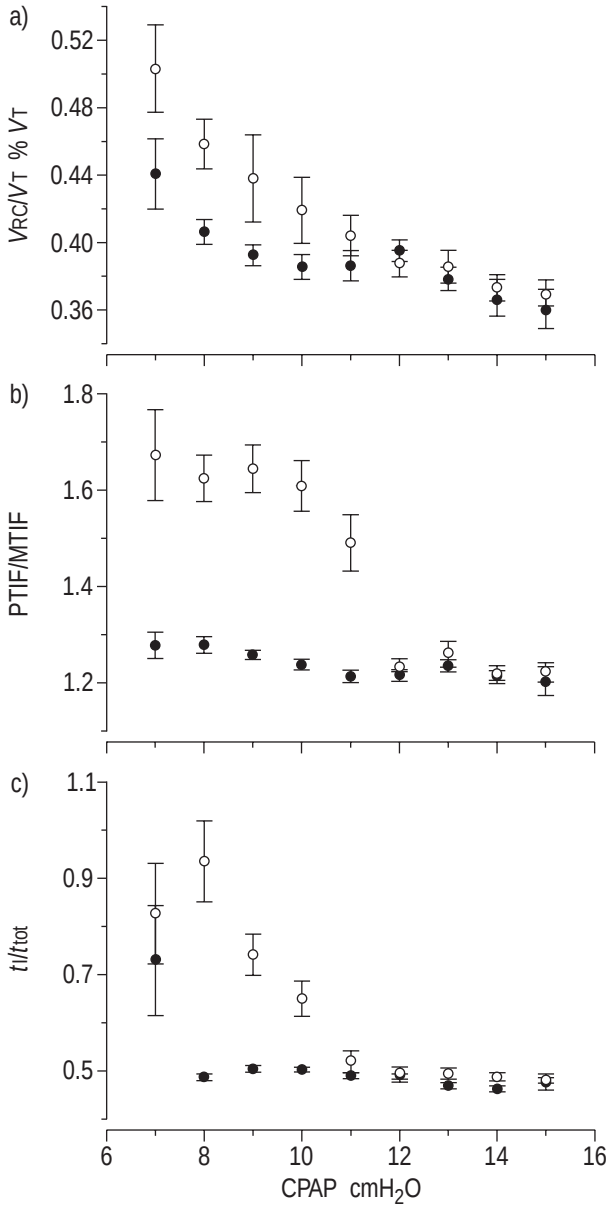

Fig. 4. – Plots of mean values (error bars represent SE) of a) fractional inspiratory time (t_I/t_{tot}); b) peak tidal inspiratory to mean tidal inspiratory flow ratio (PTIF/MTIF) and c) Rib cage contribution to tidal volume (V_{RC}/V_T), derived by respiratory inductive plethysmography and computed during three ascending (○), and three descending (●) CPAP titration runs in a representative patient. Note the hysteresis of the effect of CPAP on breathing pattern parameters.

During ascending and descending phases of CPAP titration runs RIP derived breathing patterns tracked changes in the extent of inspiratory flow limitation. The phenomenon of hysteresis in relation to changes in CPAP levels (fig. 3) is consistent with earlier reports [23].

Computer assisted RIP for detection of inspiratory flow limitation

Since visual analysis of breathing patterns is time consuming and has the potential for observer bias computerized analysis of RIP recordings was employed. Systematic

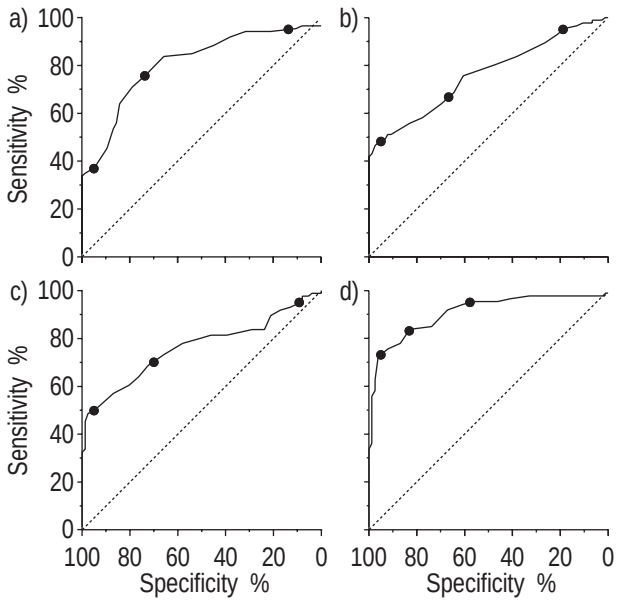

Fig. 5. – Receiver operating characteristics (ROC) curves of respiratory inductive plethysmography derived parameters for the discrimination of presence from absence of inspiratory flow limitation as defined by pressure and flow recordings in the learning sessions. a) fractional inspiratory time (area 0.81; 95% confidence interval (CI) 0.75–0.87); b) peak tidal inspiratory to mean tidal inspiratory flow ratio (area 0.76; 95% CI 0.69–0.83); c) ribcage contribution to tidal volume (area 0.76; 95% CI 0.69–0.83); and d) inspiratory flow limitation index (RIP) (area 0.90; 95% CI 0.85–0.95). The points indicate 95% sensitivity, 95% specificity and equal sensitivity and specificity and represent values of a) 0.36, 0.49, and 0.43; b) 1.20, 1.47, and 1.33; c) 0.15, 0.56, and 0.49; and d) 0.41, 0.52, and 0.48. The diagonal delineates an area of 0.5, corresponding to that achieved by chance.

evaluation in the learning sessions identified several parameters reflecting timing (t_I/t_{tot}), flow-time contour (PTIF/MTIF), configuration of the flow-volume loop (IE50), and breathing efforts (V_{RC}/V_T, LBI) that discriminated presence from absence of inspiratory flow limitation (table 2).

The values of these parameters showed considerable intra- and inter-subject variability, even at a similar degree of inspiratory flow limitation as determined by pressure and flow analysis. To obtain more stable estimates of flow limitation by RIP, the three parameters with the highest areas under the ROC curves for each breathing pattern component, *i.e.*, t_I/t_{tot}, PTIF/MTIF, and V_{RC}/V_T, (table 2) were combined to a flow limitation index. It was the most reliable measure of inspiratory flow limitation since its area under the ROC curve of 0.90 exceeded the areas of its individual components (table 2).

The concepts underlying the detection of inspiratory flow limitation by RIP were corroborated by prospective validation in another group of patients. In these tests, the accuracy to detect inspiratory flow limitation by t_I/t_{tot}, PTIF/MTIF, and V_{RC}/V_T individually, and combined to the IFL-Index(RIP), was similar to that in the training sessions (tables 2 and 3, figure 5). Changes in body position in the nonrestrained patients, did not affect diagnostic performance of the IFL-Index(RIP) since areas under the ROC curves analyzed separately for lateral and supine body position were not significantly different.

The sensitivity and specificity of the IFL-Index(RIP) were 80% and 80% at the cut-off value of 0.47. This

Table 3. – Validation sample: respiratory inductive plethysmography derived breathing pattern parameters for detection of inspiratory flow limitation

Breathing pattern parameter	Inspiratory flow limitation by analysis of pressure and airflow		
	"Absent" (level 1+2) n=107	"Present" (levels 3+4) n=93	Discrimination n=200
$t1/t_{tot}$	0.38±0.06 (0.36–0.39)	0.46±0.05 (0.45–0.48)*	0.86 (0.81–0.91)‡
PTIF/MTIF	1.23±0.1 (1.21–1.25)	1.67±0.35 (1.6–1.75)*	0.90 (0.86–0.94)‡
V_{RC}/V_T	0.41±0.16 (0.38–0.45)	0.58±0.23 (0.53–0.63)*	0.72 (0.67–0.77)‡
IFL-Index(RIP)	0.36±0.13 (0.34–0.39)	0.79±0.28 (0.73–0.84)*	0.89 (0.85–0.93)‡

Data presented as mean±SD (95% confidence interval (CI)) or area under receiver operating characteristic curve (95% CI) from recordings in 10 patients. See methods for definition of inspiratory flow limitation levels 1–4 based on airflow and pressure analysis. *: $p<0.05$ *versus* "absent" flow limitation; ‡: 95% CI not overlapping 0.5. The inspiratory flow limitation index [IFL-Index(RIP)] contains combined information from the other 3 parameters listed individually, see text for description.

compares favourably with the sensitivity and specificity of 76% reported for the IE50 ratio derived from flow-volume loops recorded by a flow meter [18], and with sensitivities and specificities at the points of equality of 82%, 76%, and 71% achieved by analysis of the pneumotachographic flow curve, the nasal pressure curve, and the differentiated RIP sum signal, respectively, in habitual snorers [9]. The superior accuracy of RIP to differentiate flow limitation levels 1 and 2 from levels 3 and 4 in the current as compared to the latter study [9] may relate to differences in signal analysis. In particular, our IFL-Index(RIP) is based not only on characteristics of the differentiated RIP sum signal, but reflects breathing efforts as well by inclusion of a parameter that represents synchronization of rib cage-abdominal motion (V_{RC}/V_T) and includes a respiratory timing parameter (t_I/t_{tot}). In contrast to an index derived from the nasal pressure curve [9], the RIP derived parameters proposed for automatic detection of inspiratory flow limitation are not expressed relative to an individual baseline nor are they based on the premise of an exclusive nasal route of breathing. All three parameters incorporated into the IFL-Index(RIP) are available

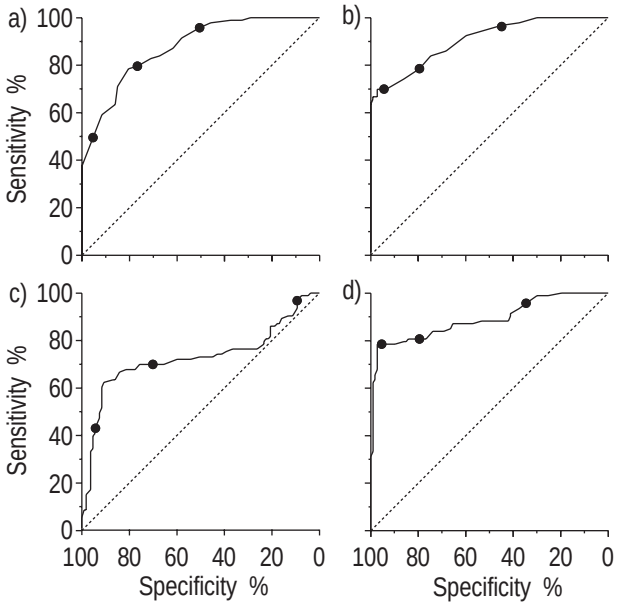

Fig. 6. – Prospective validation of the receiver operating characteristic (ROC) curves of respiratory inductive plethysmography derived parameters for the discrimination of presence from absence of inspiratory flow limitation: a) fractional inspiratory time (area 0.86; 95% confidence interval (CI) 0.81–0.91); b) peak tidal inspiratory to mean tidal inspiratory flow ratio (area 0.90; 95% CI 0.86–0.94); c) ribcage contribution to tidal volume (area 0.72; 95% CI 0.67–0.77); and d) inspiratory flow limitation index (RIP) (area 0.89; 95% CI 0.85–0.93). The points indicate 95% sensitivity, 95% specificity, and sensitivity and specificity and represent values of a) 0.38, 0.48 and 0.43; b)1.24, 1.40 and 1.32; c) 0.18, 0.64 and 0.49; and d) 0.29, 0.55 and 0.47. The diagonal delineates an area of 0.5 corresponding to that achieved by chance.

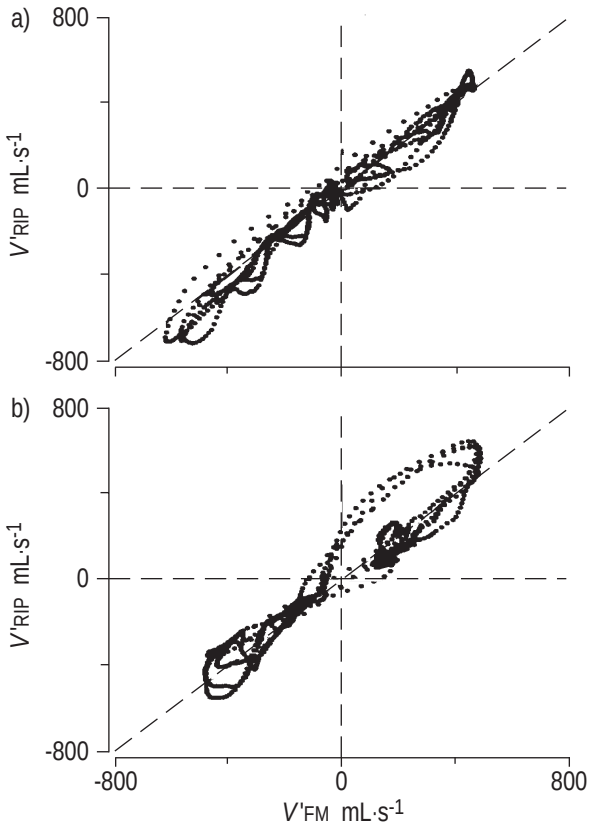

Fig. 7. – Point by point comparisons of V'_{RIP} *versus* V'_{FM} sampled at 50 Hz. a) corresponds to a period of several breaths without inspiratory flow limitation. The flow values by both methods fall near to the line of identity (dotted). b) depicts data from a period of inspiratory flow limitation (corresponding to d and h in figure 2). V'_{RIP} exceed V'_{FM} values during a significant portion of inspiration (positive values) and expiration (negative values). This is consistent with gas decompression/compression and chest wall deformation during loaded inspiration and active expiration.

after QDC during natural breathing [12]. Therefore, the IFL-Index(RIP) is not dependent on calibration of RIP in absolute volume units by means of a spirometer or flow meter.

Conclusions

It is concluded that breathing patterns recorded by respiratory inductive plethysmography undergo characteristic changes during inspiratory flow limitation. Computer assisted analysis of these waveforms provides a noninvasive means for automated detection of inspiratory flow limitation without requirement for airway instrumentation. This makes respiratory inductive plethysmography a particularly suitable tool for the study of subtle breathing disturbances during sleep.

Acknowledgements. The authors appreciate the helpful suggestions of S. Parthasarathy, Chicago, regarding oesophageal pressure measurements, and the assistance by Y. Li, Zürich, in performance of the sleep studies.

References

1. American Sleep Disorders Association Standards of Practice Committee. Practice parameters for the indications for polysomnography and related procedures. *Sleep* 1997; 20: 406–422.
2. Montserrat JM, Farré R, Ballester E, Felez MA, Pastó M, Navajas D. Nasal prongs for detection of airflow. *Am J Respir Crit Care Med* 1997; 155: 211–215.
3. Skatrud JB, Dempsey JA. Airway resistance and respiratory muscle function in snorers during NREM sleep. *J Appl Physiol* 1985; 59: 328–335.
4. Hudgel DW, Hendricks C, Hamilton HB. Characteristics of the upper airway pressure-flow relationship during sleep. *J Appl Physiol* 1988; 64: 1930–1935.
5. Guilleminault C, Stoohs R, Clerk A, Cetel M, Maistros P. A cause of excessive daytime sleepiness. The upper airway resistance syndrome. *Chest* 1993; 104: 781–787.
6. Bloch KE, Li Y, Sackner MA, Russi EW. Breathing patterns during sleep disruptive snoring. *Eur Respir J* 1997; 10: 576–586.
7. Tobin MJ, Perez W, Guenther SM, Lodato RF, Dantzker DR. Does rib cage-abdominal paradox signify respiratory muscle fatigue? *J Appl Physiol* 1987; 63: 851–860.
8. Montserrat JM, Ballester E, Olivi H, *et al*. Time-course of stepwise CPAP titration. Behavior of respiratory and neurological variables. *Am J Respir Crit Care Med* 1995; 152: 1854–1859.
9. Clark SA, Wilson CR, Satoh M, Pegelow D, Dempsey JA. Assessment of inspiratory flow limitation invasively and noninvasively during sleep. *Am J Respir Crit Care Med* 1998; 158: 713–722.
10. Buess C, Pietsch P, Guggenbuhl W, Koller EA. A pulsed diagonal-beam ultrasonic airflow meter. *J Appl Physiol* 1986; 61: 1195–1199.
11. Baydur A, Behrakis PK, Zin WA, Jaeger M, Milic-Emili J. A simple method for assessing the validity of the oesophageal balloon technique. *Am Rev Respir Dis* 1982; 126: 788–791.
12. Sackner MA, Watson H, Belsito AS, *et al*. Calibration of respiratory inductive plethysmograph during natural breathing. *J Appl Physiol* 1989; 66: 410–420.
13. Rechtschaffen A, Kales A. A manual of standardized terminology, techniques and scoring system for sleep stages of human subjects. Washington, D.C.: Public Health Service, U.S. Government Printing Office, 1968.
14. Sleep Disorders Atlas Task Force of ASDA. EEG arousals: Scoring rules and examples. *Sleep* 1992; 15: 174–184.
15. Bloch KE, Li Y, Zhang J, *et al*. Effect of surgical volume reduction on breathing patterns in severe pulmonary emphysema. *Am J Respir Crit Care Med* 1997; 156: 553–560.
16. Reich O, Brown K, Bates JHT. Breathing patterns in infants and children under halothane anesthesia: effect of dose and CO_2. *J Appl Physiol* 1994; 76: 79–85.
17. Agostoni E, Magnoni P. Deformations of the chest wall during breathing efforts. *J Appl Physiol* 1966; 21: 1827–1832.
18. Sériès F, Marc I. Accuracy of breath-by-breath analysis of flow-volume loop in identifying sleep-induced flow-limited cycles in sleep apnoea-hypopnoea syndrome. *Clin Sci* 1995; 88: 707–712.
19. Dubois AB. Resistance to breathing. *In*: Fenn WO, Rahn H, eds. Handbook of Physiology. Washington, D.C., Waverly Press Inc, 1964; pp. 451–462.
20. Gardner MJ, Altman DG. Statistics with confidence. London, British Medical Journal, 1989.
21. Hanley JA, McNeil BJ. The meaning and use of the area under a receiver operating characteristic curve. *Radiology* 1982; 143: 29–36.
22. Gleeson K, Zwillich CW, White DP. The influence of increasing ventilatory effort on arousal from sleep. *Am Rev Respir Dis* 1990; 142: 295–300.
23. Condos R, Norman RG, Krishnasamy I, Peduzzi N, Goldring RM, Rappoport DM. Flow limitation as a noninvasive assessment of residual upper-airway resistance during continuous positive airway pressure therapy of obstructive sleep apnoea. *Am J Respir Crit Care Med* 1994; 150: 475–480.
24. Sackner MA, Rao ASV, Birch S, Atkins N, Gibbs L, Davis B. Assessment of time-volume and flow-volume components of forced vital capacity. *Chest* 1982; 82: 272–278.
25. Ingram RH, Schiller DP. Effect of gas compression on pulmonary pressure, flow and volume relationship. *J Appl Physiol* 1966; 21: 1821–1826.
26. Goldman MD, Pagani M, Trang HTT, Praud JP, Sartene R, Gaultier C. Asynchronous chest wall movements during non-rapid eye movement sleep in children with bronchopulmonary dysplasia. *Am Rev Respir Dis* 1993; 147: 1175–1184.